LAWRENCE
LIVERMORE
NATIONAL
LABORATORY

LLNL-PROC-422850

Detailed Chemical Kinetic Reaction Mechanism for Biodiesel Components Methyl Stearate and Methyl Oleate

C. Naik, C. K. Westbrook, O. Herbinet, W. J. Pitz, M. Mehl

January 25, 2010

The 33rd International Symposium on Combustion
Beijing, China
August 1, 2010 through August 6, 2010

Disclaimer

This document was prepared as an account of work sponsored by an agency of the United States government. Neither the United States government nor Lawrence Livermore National Security, LLC, nor any of their employees makes any warranty, expressed or implied, or assumes any legal liability or responsibility for the accuracy, completeness, or usefulness of any information, apparatus, product, or process disclosed, or represents that its use would not infringe privately owned rights. Reference herein to any specific commercial product, process, or service by trade name, trademark, manufacturer, or otherwise does not necessarily constitute or imply its endorsement, recommendation, or favoring by the United States government or Lawrence Livermore National Security, LLC. The views and opinions of authors expressed herein do not necessarily state or reflect those of the United States government or Lawrence Livermore National Security, LLC, and shall not be used for advertising or product endorsement purposes.

Detailed Chemical Kinetic Reaction Mechanism for Biodiesel Components Methyl Stearate and Methyl Oleate

C. Naik#, C.K. Westbrook*, O. Herbinet†, W.J. Pitz* and M. Mehl*

Reaction Design Inc., San Diego, CA USA
* Lawrence Livermore National Laboratory, Livermore, CA USA
† CNRS, Nancy Universite-ENSIC, Nancy, France

Charles K. Westbrook, Corresponding Author
Lawrence Livermore National Laboratory, L-342
P.O. Box 808
Livermore, CA 94550

email: westbrook1@llnl.gov
Telephone: 1-408-897-3144

Colloquium: Reaction Kinetics

Paper length Calculation

Text:	3018
References:	560
Equations:	0
Figure 1: (72 mm+10)x2.2 + 9	189
Figure 2: (32 mm+10)x2.2 + 47	139
Figure 3: (94 mm+10)x2.2 + 31	260
Figure 4: (40 mm+10)x2.2 +31	141
Figure 5: (45 mm+10)x2.2 +27	148
Figure 6: (73 mm+10)x4.4 + 16	381
Figure 7: (80 mm+10)x4.4 +8	404
Figure 7: (87 mm+10)x4.4 +16	443
Table 1: (23 mm+10)x2.2 + 9	82
Total:	5765 words

We agree to pay for color reproduction charges if applicable.

Keywords: Kinetic Mechanisms, Oxidation, Biofuels

Detailed Chemical Kinetic Reaction Mechanism for Biodiesel Components Methyl Stearate and Methyl Oleate

C. Naik#, C.K. Westbrook*, O. Herbinet†, W.J. Pitz* and M. Mehl*

Reaction Design Inc., San Diego, CA USA
* Lawrence Livermore National Laboratory, Livermore, CA USA
† CNRS, Nancy Universite-ENSIC, Nancy, France

Abstract

New chemical kinetic reaction mechanisms are developed for two of the five major components of biodiesel fuel, methyl stearate and methyl oleate. The mechanisms are produced using existing reaction classes and rules for reaction rates, with additional reaction classes to describe other reactions unique to methyl ester species. Mechanism capabilities were examined by computing fuel/air autoignition delay times and comparing the results with more conventional hydrocarbon fuels for which experimental results are available. Additional comparisons were carried out with measured results taken from jet-stirred reactor experiments for rapeseed methyl ester fuels. In both sets of computational tests, methyl oleate was found to be slightly less reactive than methyl stearate, and an explanation of this observation is made showing that the double bond in methyl oleate inhibits certain low temperature chain branching reaction pathways important in methyl stearate. The resulting detailed chemical kinetic reaction mechanism includes more approximately 3500 chemical species and more than 17,000 chemical reactions.

1. INTRODUCTION

Biofuels have the potential to supplement conventional petroleum-based transportation fuels. Such fuels can reduce dependence on imported petroleum fuels and, since they are derived from renewable sources, can reduce net emissions of greenhouse gases. An important class of biodiesel fuels consist of long-chain monoalkyl esters of fatty acids from vegetable oils and animal fats, and currently soy oil and rapeseed oil represent major sources of these oils. Use of biodiesel in diesel engines can decrease emissions of CO, unburned hydrocarbons, and soot [1-4]. The principal components of both soy and rapeseed oil methyl ester fuels are the same five saturated and unsaturated methyl esters, methyl palmitate ($C_{17}H_{34}O_2$), methyl stearate ($C_{19}H_{38}O_2$), methyl oleate ($C_{19}H_{36}O_2$), methyl linoleate ($C_{19}H_{34}O_2$) and methyl linolenate ($C_{19}H_{32}O_2$), with structures summarized in Fig. 1. Their average compositions in soybean and rapeseed biodiesel fuels are given in Table I [5]. It is important to note that the most common components of these fuels are the molecules with one or two double bonds within the long carbon chain.

While numerous kinetic modeling studies of smaller methyl esters have been carried out [6-13], few studies of large methyl ester fuels have appeared. Dagaut et al. [14] studied the oxidation of rapeseed methyl ester fuel in a jet-stirred reactor lean at 10 atm pressure. At that time, no large alkyl ester kinetic mechanism was available, so they used a mechanism for n-hexadecane [15] to analyze their results, with good overall agreement between computed and measured concentrations of species common to both mechanism and experimental data.

Herbinet et al. [16] developed a kinetic reaction mechanism for the saturated methyl ester fuel methyl decanoate ($C_{11}H_{22}O_2$), establishing that a mechanism for such fuels could be

constructed using the same reaction classes and reaction rate models developed for n-heptane and iso-octane [17,18], with suitable additions to accommodate the methyl ester group in the molecule. The same reaction classes and rate rules used in the methyl decanoate mechanism can then be extended to larger methyl esters.

Based on their previous works on alkanes [19] and the success of the methyl decanoate mechanism [16], the Nancy combustion group updated the reaction pathway and rate rules used by the software EXGAS, for the automatic generation of detailed kinetic models, for methyl and ethyl esters, leading to their application to mechanisms for methyl and ethyl butanoates [13] and larger methyl esters up to methyl decanoate [20] and methyl palmitate [21].

Since the most common components of biodiesel fuel contain double carbon bonds, we have examined how the reaction classes and reaction rate rules can accommodate kinetics involved with double bonds in site-specific rate expressions. Zhang et al. [22] compared the reaction of saturated and unsaturated C_9 methyl esters in a motored engine, finding less reactivity from the unsaturated fuel under similar operating conditions. They reasoned that the presence of the double bond in the unsaturated fuel reduces the rates of radical isomerization rates that normally accelerate the overall rate of low temperature combustion. Experimental studies by Vanhove et al. [23] of low temperature ignition of isomers of hexene in a rapid compression machine showed that the location of the double bond in the hexene isomer played an important role in determining overall reactivity. They found that 1-hexene had low temperature reactivity similar to the saturated n-hexane, while 2-hexene had less low T reactivity, and in 3-hexene, the low temperature reactivity almost disappeared. Kinetic

modeling analyses by Bounaceur et al. [24] and Mehl et al. [25] reproduced the results of Vanhove et al. by reducing significantly the rates of alkyl and alkylperoxy radical isomerization reactions when the cyclic transition state has an imbedded double bond. Based on these recent studies, mechanisms were developed by Herbinet et al. [26] for two unsaturated fuels based on methyl decanoate, with double bonds located at two different locations in the carbon chain. One conclusion of that work was that the overall reactivity of methyl-5-decenoate, with the double bond in the middle of the carbon chain, was significantly less than the reactivity of methyl-9-decenoate, especially in the low temperature region, and that the reduced reactivity could be attributed to significantly reduced rates of RO_2 isomerization in the methyl-5-decenoate.

In the present work, we have extended these kinetic approaches to develop a kinetic reaction mechanism for two of the C_{19} components of soy and rapeseed biodiesel fuel. These two species, methyl stearate and methyl oleate, provide important capabilities required to understand and predict the combustion of biodiesel fuels and differences between the kinetic properties of the saturated and unsaturated components. The resulting kinetic mechanism is quite large (more than 3500 chemical species and more than 17,000 elementary reactions), and considerable mechanism reduction is likely to be needed for use of such a mechanism in practical simulation analyses. However, a fundamentally based and tested fully detailed mechanism can lead to a reliable reduced mechanism with much greater validity than any other method.

2. REACTION MECHANISM

The detailed kinetic mechanism for methyl stearate and methyl oleate is based on the reaction pathways and rate rules developed originally for alkane fuels by Curran et al. [14,15], with modifications for alkyl esters by Herbinet et al. [21,26] . The presence of the methyl ester group modifies C - H bond strengths adjacent to the ester group, which modifies the rate of their H atom abstraction reactions. In addition, H atom abstraction reaction rates in methyl oleate are included in a complete site-specific approach, in contrast with our original mechanisms which treated olefins in a lumped approximation. In the vicinity of the double bond in methyl oleate, there are additional types of C-H bonds, including vinylic and allylic bonds, which are reflected in modified H atom abstraction and molecular decomposition reaction rates. These modifications in C-H bond strengths in methyl stearate and methyl oleate are illustrated in Fig. 2.

We have included addition reactions of O_2 to alkyl-like radicals produced via H atom abstraction from methyl stearate and to alkenyl-like radicals from methyl oleate. Subsequent RO_2 isomerization reaction pathways, including the full variety of low temperature hydrocarbon oxidation reaction pathways that lead to low temperature ignition and negative temperature coefficient (NTC) behavior are also included for methyl stearate and oleate, subject to the modifications noted above when isomerization reactions take place across a double bond. Due to the presence of the methyl ester group and, in the case of methyl oleate, the double bond within the C atom chain, the reaction rate rules originally developed only for saturated alkane fuels required considerable enhancements. All of these features are adopted from our recent methyl decanoate and methyl decenoate studies [21,26], where more thorough descriptions

may be found. We have included these reaction pathways for methyl oleate since it is a major fuel component, but these low temperature reaction pathways have not been included in the present reaction mechanism for any other olefin-like intermediates that can be produced from methyl stearate. Similarly, the same low temperature submechanisms are not included for any alkyne intermediates, although future extensions of the present approach to include submechanisms for methyl linoleate and methyl linolenate will require such submechanisms.

3. RESULTS

There are two general classes of experiments that have produced data that can be used to validate the present kinetic mechanisms, specifically shock tube ignition delay times and jet-stirred reactor combustion experiments. In the absence of experimental results for either methyl stearate or methyl oleate in the jet-stirred reactor, we carried out calculations in which each methyl ester was used as the only fuel, and the computed results were compared with the rapeseed methyl ester (RME) experiments of Dagaut et al. [14] at 10 atm pressure and temperatures from 800K to 1400K. Simulations included data from experiments at equivalence ratios of 0.5 and 1.0.

Overall, the agreement between computed and experimental results, using both methyl stearate and methyl oleate as fuels, is very good for both lean and stoichiometric cases, as illustrated in Figs. 3 (for ϕ = 1.0) and 4 (for ϕ = 0.5). In these figures, the symbols show the measured concentrations at selected reactor temperatures, the solid curves show the computed results when methyl stearate is the fuel, and the dotted curves show the computed

results with methyl oleate is the fuel. The two fuels show very nearly the same reactivity, but all the results indicate that methyl oleate has slightly less reactivity under these conditions than methyl stearate. This can be seen in Fig. 3 where the O_2 consumption rate is slightly slower with methyl oleate, and the production rates of all of the intermediates and CO_2 are slightly less when methyl oleate is the fuel than for methyl stearate. It is worth noting that the level of agreement is only slightly better than that reported by Dagaut et al. [14] who simulated the same experiments using an n-hexadecane reaction mechanism. The only area in which one should expect significantly better results from the methyl ester mechanisms is for CO and CO_2 at low temperatures, where the methyl ester group produces these species very early during the oxidation process [4], but the current results are only moderately improved over those reported by Dagaut et al. In addition, the largest 1-olefin reported by Dagaut et al. was 1-hexene, for which their n-hexadecane mechanism overpredicted the measured values by about a factor of 5 in the stoichiometric case. The present methyl ester mechanisms reduces that overprediction by about one half, which can be attributed to the fact that the lack of symmetry in the methyl ester molecule relative to n-hexadecane reduces the number of reaction pathways leading to all large 1-olefins in both methyl esters. Since RME contains about 60% methyl oleate and only about 2% methyl stearate, we should expect the methyl oleate computed results to be a more accurate simulation for the RME experiments.

We used the methyl ester mechanisms to predict their ignition delay times for a class of shock tube problems that has been used widely to study the influence of molecular structure on ignition. The original experiments were carried out by Adomeit et al. [27-29] and examined

n-heptane, n-decane and iso-octane ignition at pressures of 13.5 and 40 bar pressure over a range of temperatures that included the region of negative temperature coefficient (NTC). They found that the n-alkanes ignited at very nearly the same rates over the entire temperature range, while iso-octane was considerably slower to ignite within the narrower temperature range from about 700K to 900K. The computed results for methyl stearate and methyl oleate are shown as lines in Fig. 5 and both show a distinct region of NTC behavior over the same range of temperatures as those seen experimentally. The experimental results for n-heptane and n-decane are shown as symbols in Fig. 5, and computed results [30] are shown for n-hexadecane, which has nearly the same C chain length as these methyl esters. The similarities between all the n-alkanes are evident, and the methyl ester mechanisms show that methyl oleate is moderately less reactive than methyl stearate only in the NTC region. It appears that the C=C double bond in the middle of the methyl oleate molecule is indeed reducing its overall rate of alkylperoxy radical isomerization, when compared to methyl stearate. As noted above, the double bond is assumed to reduce the rate of RO_2 and OOROOH isomerization when the double bond is imbedded in the transition state ring for these reactions, thereby reducing the overall rate of low temperature chain branching.

Further insight into the combustion kinetics of these two C_{19} esters can be seen in the reaction pathway analysis shown for methyl stearate in Fig. 6. This plot shows the fuel consumption reactions for reaction of stoichiometric fuel/air mixtures at 800K and 12 atm, at a time where 10% of the fuel has been consumed. The fraction in percent of the total fuel consumption rate is shown numerically on the figure for each reaction path. Since most of the C-H bonds in methyl stearate are the same, H atom abstraction by radicals is the same at each

of these sites. The abstraction rates of H atom in the two terminal methyl groups are slower, due to the stronger primary C-H bonds and are not shown, and the abstraction of the H atoms from the C adjacent to the carbonyl group are faster, due to this weaker C-H bond. Zhang and Boehman [31] commented on the relative importance of H atom abstraction from this a-site in alkyl ester combustion, in their case in a motored engine.

Part of the great variety of low temperature reaction pathways for these methyl esters is illustrated in Fig. 7, showing the reaction pathways that follow the abstraction of an H atom from the C adjacent to the carbonyl group in methyl stearate. As noted above, this is the largest H atom abstraction path from methyl stearate, due to this being the weakest C-H bond in the molecule. At the 800K temperature of this example, β-scission of the resulting radical is a relatively minor process, producing the alkyl radical 1-$C_{15}H_{31}$ and a small carbonyl molecule. The most important reaction of the methyl stearate radical is addition of O_2 at the radical site to produce a carbonyl version of RO_2, which then abstracts an H atom from any one of several nearby sites within the molecule. The fastest internal H atom abstractions involve 6- and 7-membered transition state rings, both of which are shown in Fig. 7. Both processes can lead to further addition of O_2 and production of multiple radical species, especially OH, which provide chain branching. Also shown in the figure is the fact that this second O_2 addition is particularly dominant in the pathway leading from the 6-membered transition state ring. Some of the smaller fragments of decomposition include radicals and stable species which lead to CO_2 at these low temperatures, which has implications for the relative inefficiency of methyl esters for soot reduction in diesel engines, when compared with other oxygenated fuels [4].

The same conditions as those in Fig. 6 lead to the flux diagram shown in Fig. 8 for methyl oleate, where the allylic and vinylic bonds change the balance in rates of H atom abstraction that was seen in the methyl stearate fluxes. Radical addition to the double bond contributes slightly to the overall rate of reaction, but most of the methyl oleate consumption again occurs via H atom abstraction. The rate of abstraction from the site adjacent to the carbonyl group is again higher than abstractions from the many secondary C-H bond sites, but abstraction from the allylic sites is even faster, and abstraction from the vinylic sites are much too slow to be shown in Fig. 8. We are using rates for these allylic and vinylic site abstraction reactions proposed by Herbinet et al. [26] and Mehl et al. [25], which lead to a total rate of fuel consumption that is nearly the same overall in the two fuels but not as evenly distributed over the fuel molecule for methyl oleate. In fact, the most favored H atom abstractions in methyl oleate are from these allylic sites, as shown in Fig. 8; subsequent addition of O_2 to these resulting allylic sites at low temperatures leads to a majority of the RO_2 species being produced close to the double bond (Note that we are using RO_2 in a more general sense than in alkane oxidation, where R is often used to represent a true alkyl radical. Here we are using R to represent a radical produced by removal of one H atom from either methyl stearate or methyl oleate). Since the rates of RO_2 isomerization reactions, which lead to most of the low temperature chain branching in these kinetic systems [17,18], are significantly reduced when a double bond is imbedded in the transition state ring, the overall rate of chain branching in methyl oleate is sharply reduced relative to that in methyl stearate. The allylic sites in methyl oleate that result from its double bond force the majority of RO2 formation to occur close to

the double bond, which then limits the subsequent rate of isomerization and reduces the overall rate of ignition relative to the saturated methyl stearate.

These kinetic features due to the presence of double bonds in methyl esters and the way they preferentially reduce the rates of chain branching sequences are responsible for the observations of Zhang et al. [22] that combustion of unsaturated C_9 esters was slower than comparable saturated esters. Sarathy et al. [32] recently studied combustion of methyl butanoate and its unsaturated analog methyl crotonate, and while they observed higher levels of unsaturated intermediate species such as acetylene in the methyl crotonate results, the two fuels burned at very nearly equal rates. That result is still consistent with the present results, since low temperature kinetic pathways do not play any significant role in the combustion rates of methyl butanoate [6,7], so suppression of alkylperoxy radical isomerization with a double bond in methyl crotonate would have little effect on their relative rates of combustion.

4. CONCLUSIONS

This study describes the development of reaction mechanisms for two related C_{19} methyl ester fuels, the saturated methyl stearate and methyl stearate, which has a double bond in the middle of the long C chain. These mechanisms were constructed using mostly existing kinetic pathway and reaction rate rules. These mechanisms are used to investigate their relative rates of combustion, with special attention to the influence of the double bond in methyl oleate. These results are consistent with previous studies by Herbinet et al. [26] and Zhang et al. [22] for combustion of other methyl esters and studies by Mehl et al. [25] and Buonaceur et al. [xx] that the double bond suppresses RO2 and OOROOH isomerization rates in which the double bond is imbedded in the transition state ring. It is expected that addition of further double bonds to the methyl ester chain, such as for other components of many biodiesel fuels including the additional components in Table 1, will lead to further inhibitions to their low temperature chain branching rates and overall reduced low temperature reaction rates.

The kinetic mechanism files for this mechanism can be obtained from the authors.

5. ACKNOWLEDGMENTS

This work was supported by the U.S. Department of Energy, Office of Freedom CAR and Vehicle Technologies, and the authors thank program manager Kevin Stork for their support of this work. This work was performed under the auspices of the U.S. Department of Energy by Lawrence Livermore National Laboratory under Contract DE-AC52-07NA27344.

References

1. A. Tsolakis, A. Megaritis, M.L. Wyszynski, and K. Theinnoi, Energy 32 (2007) 2072-2080.

2. M.E. Tat, P.S. Wang, J.H. Van Gerpen, and T.E. Clemente, J. Am. Oil Chem. Soc. 84 (2007) 865-869.

3. R.L. McCormick, J.D. Ross, and M.S. Graboski, Environ. Sci. Technol. 21 (4)(1997) 1144-1150.

4. C.K. Westbrook, W.J. Pitz, and H.J. Curran, J. Phys. Chem. A 110 (2006) 6912-6922.

5. J. Van Gerpen, B. Shanks, R. Pruszko, D. Clements, and G. Knothe, Biodiesel production technology, National Renewable Energy Laboratory subcontractor report NREL/SR-510-36244, 2004.

6. E.M. Fisher, W.J. Pitz, H.J. Curran, and C.K. Westbrook, Proc. Combust. Inst. 28 (2000) 1579-1586.

7. S. Gaïl, M.J. Thomson, S.A. Syed, P. Dagaut, P. Dievart, A.J. Marchese, and F.L. Dryer, Proc. Combust. Inst. 31 (2007) 305-311.

8. A. Farooq, D.F. Davidson, R.K. Hanson, L.K. Huynh, and A. Violi, Proc. Combust. Inst. 32 (2009) 247-253.

9. W.K. Metcalfe, C. Togbé, P. Dagaut, H.J. Curran, and J.M. Simmie, Combust. Flame 156 (2009) 250-260.

10. L. Gasnot, V. Decottignies, and J.F. Pauwels, Fuel 84 (2005) 505-518.

11. S.M. Walton, M.S. Wooldridge, and C.K. Westbrook, Proc. Combust. Inst. 32 (2009) 255-262.

12. C.K. Westbrook, W.J. Pitz, P.R. Westmoreland, F.L. Dryer, M. Chaos, P. Osswald, K. Kohse-Höinghaus, T.A. Cool, J. Wang, B. Yang, N. Hansen, and T. Kasper, Proc. Combust. Inst. 32 (2009) 221-228.

13. M.H. Hakka, H. Bennadji, J. Biet, M. Yahyaoui, V. Warth, L. Coniglio, P.A. Glaude, F. Billaud, F. Battin-Leclerc, Int. J. Chem. Kin., (2009), in press

14. P. Dagaut, S. Gaïl, and M. Sahasrabudhe, Proc. Combust. Inst. 31 (2007) 2955-2961.

15. A. Ristori, P. Dagaut, M. Cathonnet, Combust. Flame 125 (2001) 1128-1137.

16. O. Herbinet, W.J. Pitz, and C.K. Westbrook, Combust. Flame 154 (2008) 507-528.

17. H.J. Curran, P. Gaffuri, W.J. Pitz, and C.K. Westbrook, Combust. Flame 114 (1998) 149-177.

18. H.J. Curran, P. Gaffuri, W.J. Pitz, and C.K. Westbrook, Combust. Flame 129 (2002) 253-280.

19. J.Biet, M.H. Hakka, V. Warth, P.A. Glaude, F. Battin-Leclerc, Energy and Fuel, 22 (2008) 2258-2269.

20. P.A. Glaude, O. Herbinet, S. Bax, J. Biet, V. Warth, F. Battin-Leclerc, Combust. Flame (2010) submitted.

21. O. Herbinet, J. Biet, H.M. Hakka, V. Warth, P.A. Glaude, A. Nicolle, F. Battin-Leclerc, Proc. Combust. Inst. 33 (2010) submitted.

22. Y. Zhang, Y. Yang, and A.L Boehman, Combust. Flame 156 (2009) 1202-1213.

23. G. Vanhove, M. Ribaucour, and R. Minetti, Proc. Combust. Inst. 30 (2005) 1065-1072.

24. R. Bounaceur, V. Warth, B. Sirjean, P.A. Glaude, R. Fournet, and F. Battin-Leclerc, Proc. Combust. Inst. 32 (2009) 387-394.

25. M. Mehl, G. VanHove, W.J. Pitz, and E. Ranzi, Combust. Flame 155 (2008)756-772.

26. O. Herbinet, W.J. Pitz, and C.K. Westbrook, Combust. Flame (2009) doi: 10.1016/j.combustflame.2009.10.013

27. H.K. Ciezki, G. Adomeit, Combust. Flame 93 (1993) 421-433.

28. K. Fieweger, R. Blumenthal, G. Adomeit, Combust. Flame 109 (1997) 599-619.

29. U. Pfahl, K. Fieweger, G. Adomeit, Proc. Combust. Inst. 26 (1996) 781-789.

30. C.K. Westbrook, W.J. Pitz, O. Herbinet, H.J. Curran, E.J. Silke, Combust. Flame 156 (2009) 181-199.

31. Y.Zhang, A.L. Boehman, Combust. Flame (2009) doi:10.1016/j.combustflame.2009.09.003.

32. S.M. Sarathy, S. Gail, S.A. Syed, M.J. Thomson, P. Dagaut, Proc. Combust. Inst. 31 (2007) 1015-1022.

Table Caption

1. Average compositions (%) of soybean and rapeseed biodiesels.

Table 1:

Esters	Soybean biodiesel	Rapeseed biodiesel
methyl palmitate	6-10%	4.3%
methyl stearate	2-5%	1.3%
methyl oleate	20-30%	59.9%
methyl linoleate	50-60%	21.1%
methyl linolenate	5-11%	13.2%

FIGURE CAPTIONS

1. Major components of soy and rapeseed oil biodiesel fuel

2. Different types of H-atoms considered for the H-atom abstractions in a) methyl stearate, b) methyl oleate, and c) methyl linoleate.
   P = primary alkylic, S = secondary alkylic, SCO = secondary alkylic adjacent to the carbonyl group, AS = secondary allylic, and VT = tertiary vinylic H-atom

3. Comparisons between experiments [14] and computed species profiles in jet-stirred reactor. Experiments (symbols) used RME as fuel, computations for methyl stearate (solid lines) and methyl oleate (dashed lines), 10 bar, ϕ=1.0

4. Comparisons between experiments [14] and computed species profiles in jet-stirred reactor. Experiments (symbols) used RME as fuel, computations for methyl stearate (solid lines) and methyl oleate (dashed lines), 10 bar, ϕ=0.5

5. Autoignition of stoichiometric methyl stearate/air and methyl oleate/air at 13.5 atm. Also shown are experimental results for n-heptane/air [27], n-decane/air [29] and computed results for n-hexadecane [30].

6. Computed rates of consumption of stoichiometric methyl stearate air at 800K, 12 bar, 10% fuel consumption

7. Computed results for consumption of methyl stearate radical

8. Computed rates of consumption of stoichiometric methyl oleate air at 800K, 12 bar, 10% fuel consumption

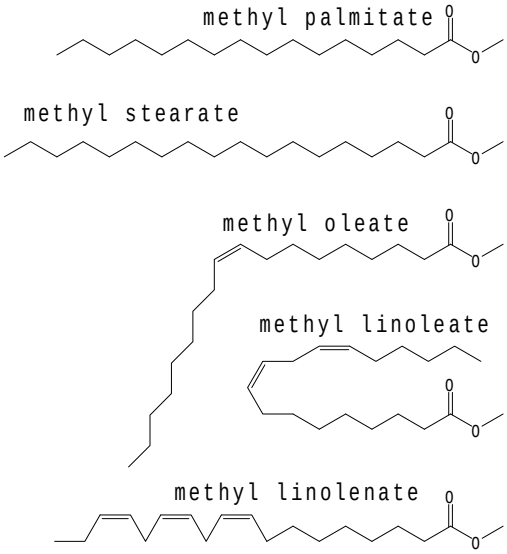
methyl palmitate
methyl stearate
methyl oleate
methyl linoleate
methyl linolenate

Figure 1

Figure 2

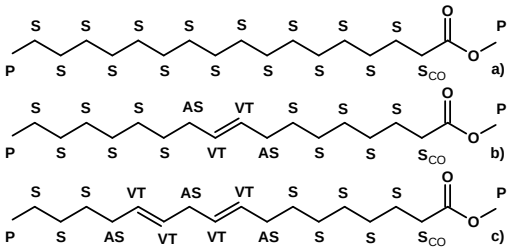
S S S S S S S S
O
P
O
P S S S S S S S SCO
a)
S S S AS VT S S S
O
P
O
P S S S VT AS S S SCO
b)
S S VT AS VT S S S
O
P
O
P S AS VT VT AS S S SCO
c)

Figure 3

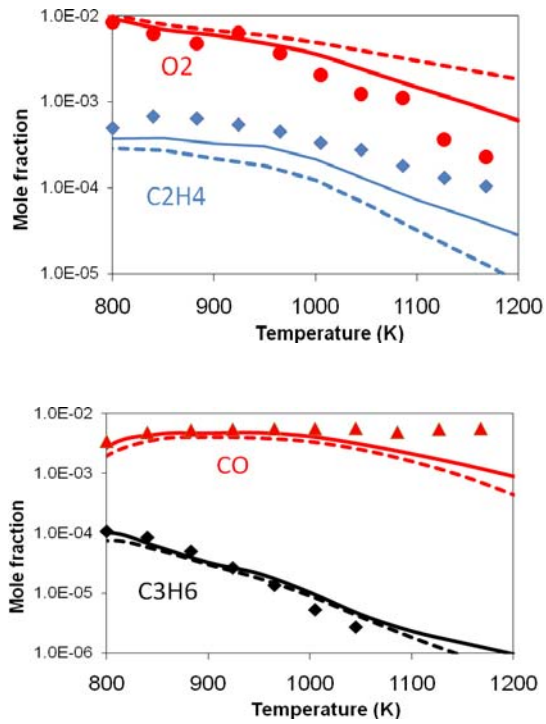
1.0E-02
1.0E-03
1.0E-04
1.0E-05
Mole fraction
O2
C2H4
800
900
1000
1100
1200
Temperature (K)
1.0E-02
1.0E-03
1.0E-04
1.0E-05
1.0E-06
Mole fraction
CO
C3H6
800
900
1000
1100
1200
Temperature (K)

Figure 4

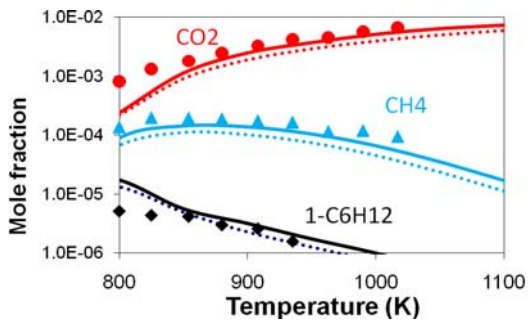
1.0E-02
1.0E-03
1.0E-04
1.0E-05
1.0E-06
Mole fraction
CO2
CH4
1-C6H12
800
900
1000
1100
Temperature (K)

Figure 5

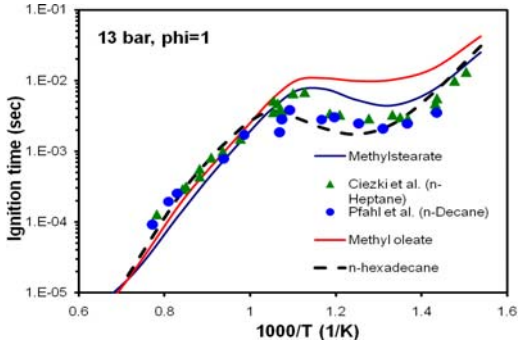
13 bar, phi=1
Ignition time (sec)
1000/T (1/K)
1.E-01
1.E-02
1.E-03
1.E-04
1.E-05
0.6
0.8
1
1.2
1.4
1.6
Methylstearate
Ciezki et al. (n-Heptane)
Pfahl et al. (n-Decane)
Methyl oleate
n-hexadecane

Figure 6

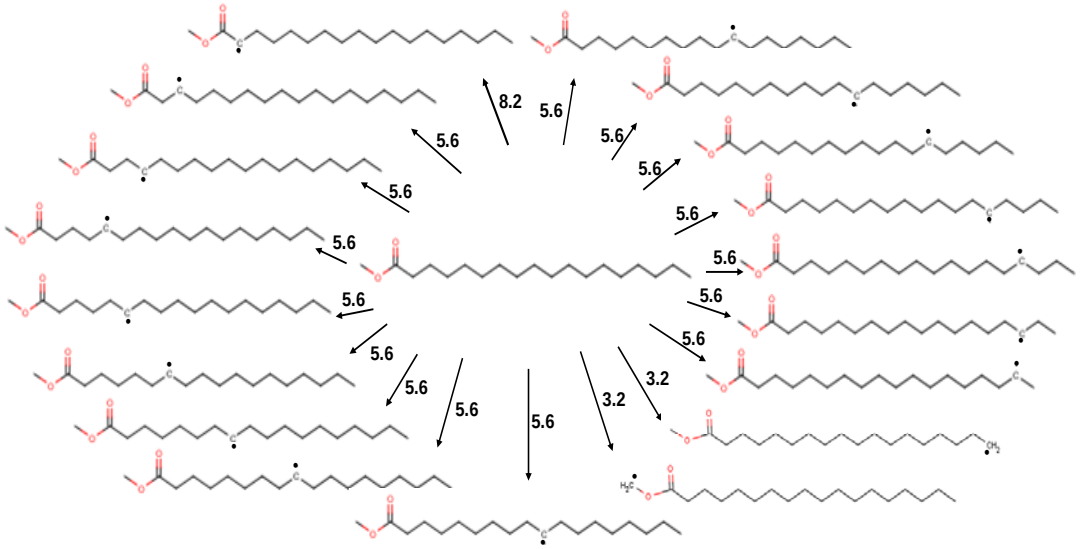

Figure 7

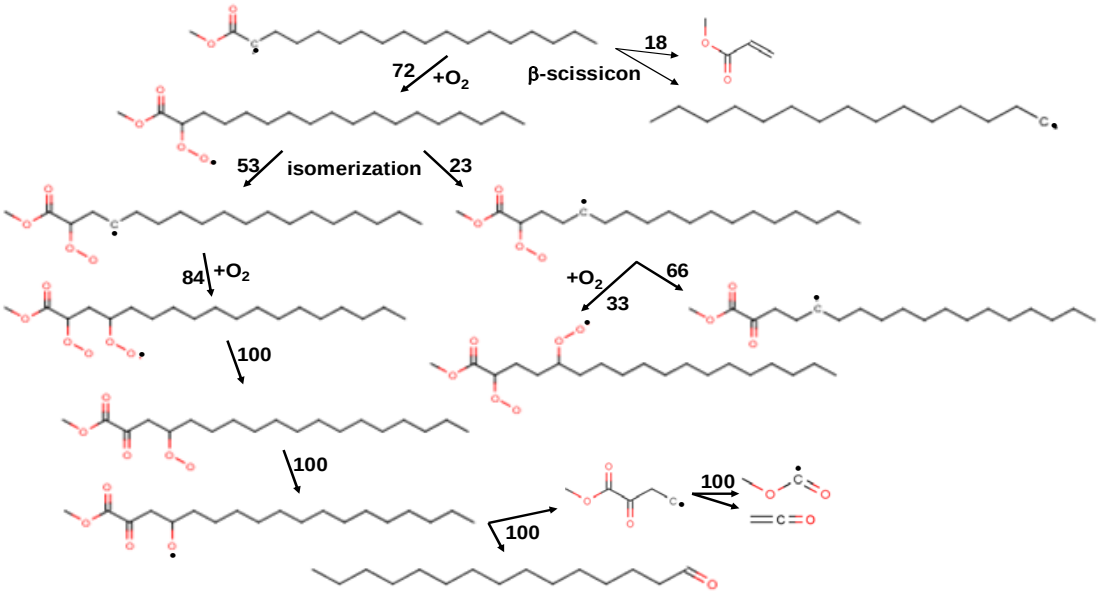
18
72
+O2
β-scissicon
53
isomerization
23
84
+O2
+O2
66
33
100
100
100
100
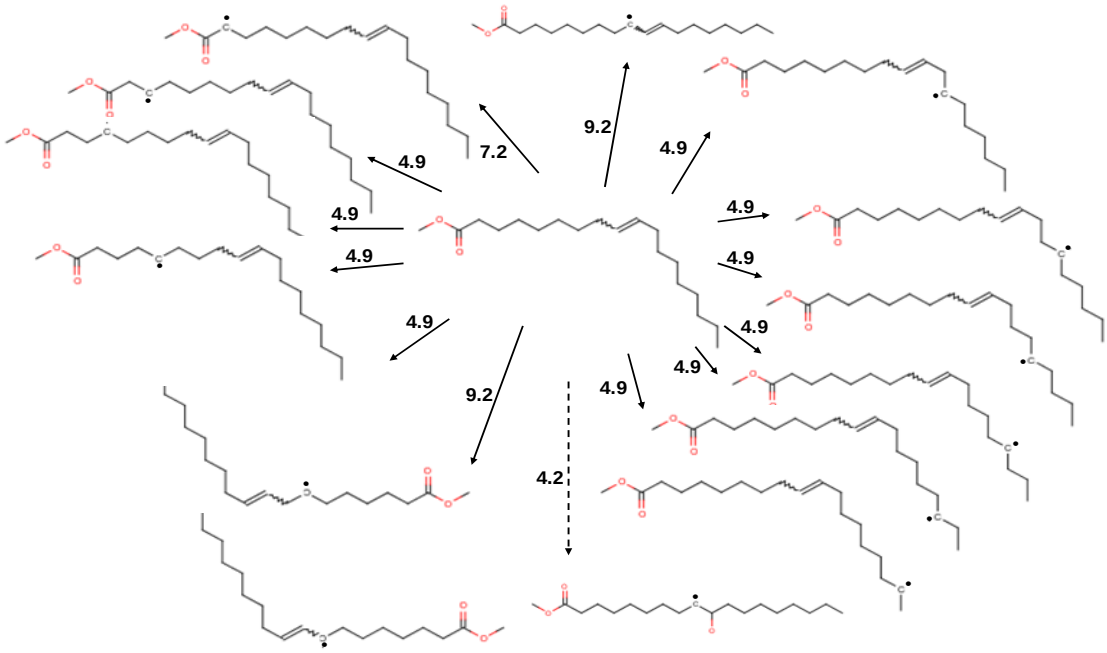
Figure 8